

Observation of the Behavior of Deuteriums Implanted in Aluminium by Use of the Nuclear Reaction $D(^3\text{He}, p)^4\text{He}$

By

Kunio HIGASHI*, Yoshio MATSUNO*, Hiroshi SAKAMOTO**,
Yasuhito MATSUI* and Haruyuki FUJITA*

(Received March 25, 1982)

Abstract

By applying the depth-profiling technique using the nuclear reaction $D(^3\text{He}, p)^4\text{He}$, the thermal behavior of deuteriums implanted in aluminium at a depth of 0–2 μm was examined.

The behavior of deuteriums depended greatly on the polishing procedures for the sample surface. When the surface was polished on a series of five abrasive papers or finished by diamond paste, the dispersion behavior of deuteriums in aluminium was quite different from that predicted on the basis of ordinary diffusion in homogeneous media. As suggested by Bugeat and Ligeon, it may be explained by the existence of a weak trapping effect against implanted deuteriums. The half-life of the trapped state at 0°C was estimated at about 1.4×10^4 sec. Once they are released from the trapping sites, they rapidly disperse over the bulk of aluminium with an ordinary diffusivity measured by permeation methods.

On the other hand, for the samples whose surface was finished with coarse Al_2O_3 , the deuterium implanted at a depth of 0–2 μm had a much smaller dispersibility than those observed for samples which were polished on a series of five abrasive papers or finished by diamond paste. At room temperature the depth profile was almost unchanged, even after a few weeks. A large depth-dependence of the dispersion behavior was observed.

I. Introduction

For the development of fusion reactors, many technical problems concerning the behavior of hydrogen isotopes in metals must be solved. The retention of the hydrogen isotopes in the material of the vacuum chamber, and their subsequent release and return to the plasma are very important for plasma parameters. Hydrogen isotopes in metals give rise to a serious problem for the structural integrity of the material because of swelling, cracking, hydrogen embrittlement and blistering.

* Department of Nuclear Engineering.

** Nippon Atomic Industry Group Co., Ltd., 4-1 Ukijima-cho, Kawasaki-ku, Kawasaki 210.

Recently, depth-profiling methods for hydrogen isotopes by the use of nuclear reactions have been developed. These ion-beam techniques have the potentiality to become useful methods for the observation of the behavior of hydrogen-isotopes in materials. The nuclear reactions of $H(t, n)^3He^{(1)}$, $H(^{11}B, \alpha)2^4He^{(2,3)}$, $D(d, n)^3He^{(4,5)}$, $D(d, p)^3T^{(6,7)}$, $D(^3He, p)^4He^{(5),8-12)}$, $H(^{19}F, \alpha r)^{16}O^{(13,14)}$, and $H(^{15}N, \alpha r)^{12}C^{(15-17)}$ have been applied for the depth-profiling.

By using the reaction $D(^3He, p)^4He$, we examined the thermal behavior of deuterium implanted in aluminium at a depth of 0–2 μm . The depth profiling was successfully carried out, and some interesting behavior of deuterium in aluminium was observed.

II. Analytical Method

Fig. 1 shows the principle of the depth-profiling method. The beam of $^3He^+$ with energy E^0 comes vertically into a metal. The incident particle is gradually decelerated along the path in the metal because of the stopping-power effect, and finally stops at the depth L . Then, the energy of 3He changes from E^0 at the surface ($x=0$) to 0 at the end of the range ($x=L$).

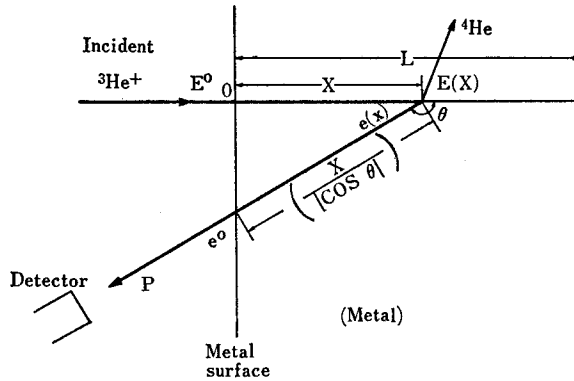


Fig. 1. Illustration for principle of depth profiling.

The energy of a proton generated by the reaction of 3He of energy $E(\leq E^0)$ with a stagnant D in the metal can be expressed by the so-called Q -equation, which is written in the present case as follows:

$$g_{\theta}(E) = 0.12E(x) \left[2 \cos^2 \theta + \frac{122.3}{E(x)} + 1.667 \right. \\ \left. + 2 \cos \theta \left\{ \cos^2 \theta + 6.667 \left(\frac{18.35}{E(x)} + 0.25 \right) \right\}^{1/2} \right]. \quad (1)$$

In the above dimensional formula, $E(x)$ has the unit of MeV. The angle θ for the

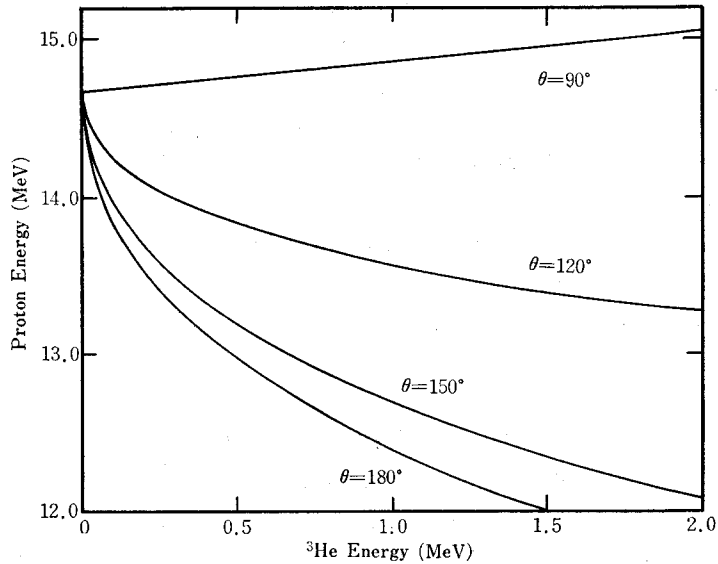


Fig. 2. Relation between emitted proton energy and incident ³He energy at laboratory emission angles.

released proton is taken in the laboratory system as shown in Fig. 1. The Q -value of the reaction $D(^3\text{He}, p)^4\text{He}$ is 18.36 MeV.

The relation between the energies of ³He and p is shown in Fig. 2 with a parameter of the angle θ . One may see in Fig. 2 that the smaller the energy of ³He, the larger the energy of p released in a backward direction. When ³He reacts with D in a deeper location in metal, the detected proton energy must be larger. Then, the proton-energy spectrum observed can be converted into a corresponding depth-profile by using the information on nuclear reaction kinematics, slowing-down of the incident and generated particles, and cross section of the reaction.

When the relation between ³He-energy E and the residual range R in the metal^{18,19)} (i.e. the range function) is written as

$$E = F(R) \quad (2)$$

$$\text{or} \quad R = F^{-1}(E) \quad (3)$$

the energy of ³He at depth x , $E(x)$, can be expressed as a function of x as follows:

$$E(x) = F\{F^{-1}(E^0) - x\} \quad (4)$$

where F^{-1} is the inverse function of F . When ³He reacts with D at depth x and a proton is released at an angle θ , the proton energy at the moment of generation, $e(x)$, is

$$e(x) = g_{\theta}\{E(x)\} = g_{\theta}[F\{F^{-1}(E^0) - x\}]. \quad (5)$$

The energetic proton is also decelerated along the path-length $x/|\cos \theta|$ before coming out of the surface. The proton energy at the surface, e^0 , is expressed by means of the range function of the proton in the metal, f , as

$$\begin{aligned} e^0(x) &= f \left[f^{-1} \{e(x)\} + \frac{x}{\cos \theta} \right] \\ &= f \left[f^{-1} \{g_0[F \{F^{-1}(E^0) - x\}]\} + \frac{x}{\cos \theta} \right]. \end{aligned} \tag{6}$$

The above expression shows that the proton energy at the surface for a fixed angle and for a given incident energy of ^3He has a unique relation to the depth at which the reaction occurred.

When the depth profile of deuterium concentration in the metal is denoted by $N(x)$ (D/cm^3), the number of protons which come out of the surface at the experimental solid angle of detection $(d\Omega)_{\text{exp}}$ after the reaction in an infinitesimal width dx around x is

$$n(e^0)de^0 = ISN(x)dx \left(\frac{d\sigma(E)}{d\Omega} \right)_{\text{lab}} \cdot (d\Omega)_{\text{exp}}. \tag{7}$$

Hence, the energy spectrum of the proton at the surface is

$$n(e^0) = \frac{ISN(x)dx \left(\frac{d\sigma(E)}{d\Omega} \right)_{\text{lab}} \cdot (d\Omega)_{\text{exp}}}{\left(\frac{de^0}{dx} \right) dx} \tag{8}$$

where I and S are the dose of ^3He per unit area and the surface area bombarded by the ^3He beam, respectively. The differential cross section of the nuclear reaction, $\sigma(E)$, is a function varying smoothly with energy²⁰⁾. The peak appears at the ^3He energy of ~ 600 keV. The reaction differential cross section converted to lab-coordinates is denoted by $(d\sigma(E)/d\Omega)_{\text{lab}}$. Because, in the energy range of $E < 1.5\text{MeV}$, the reaction of $D(^3\text{He}, p)^4\text{He}$ may be regarded as isotropical in the center-of-mass system²¹⁾, we may write²²⁾

$$\left(\frac{d\sigma(E)}{d\Omega} \right)_{\text{lab}} = \alpha \bar{\sigma}, \tag{9}$$

$$\alpha \equiv \frac{r^2 + 2r \cos \vartheta + 1}{1 + r \cos \vartheta}, \tag{10}$$

$$r \equiv \sqrt{\frac{0.375E}{E + 2.5Q}}, \tag{11}$$

$$\cos \theta = \frac{r + \cos \vartheta}{\sqrt{r^2 + 2r \cos \vartheta + 1}}, \tag{12}$$

where $\bar{\sigma}$ is the average differential cross section, ϑ is the angle in the center-of-mass system. By substituting Eq. (9) into Eq. (8), we have

$$N(x) = \frac{n(e^0) \left(\frac{de^0(x)}{dx} \right)}{IS \alpha \bar{\sigma} (d\Omega)_{\text{exp}}} \quad (13)$$

The depth x and $de^0(x)/dx$ corresponding to a given e^0 can be obtained from Eq. (6).

III. Experimental

III-1 Preparation of Aluminium Specimens for Implantation

Rod-shaped aluminium (99.999 %) of 10 mm diameter was sectioned mechanically into 2 mm thickness and annealed at 200°C for one hour. Because surface roughness leads to erroneous results in depth-profiling, the specimens were polished prior to the implantation of the deuteriums.

The thermal behavior of deuterium implanted in a near surface region depends greatly on the surface conditions. Then, the following three kinds of specimens (A, B and C) were prepared with different polishing procedures to obtain some information about their dependence.

Specimens A: Aluminium specimens were polished on a series of five abrasive-papers (#400, #800, #1000, #1200, and #1500) supplied by Sakamoto Koki Ltd..

Specimens B: After polishing on the series of five abrasive-papers above, some specimens were further polished by diamond-paste with oil. The surface appeared featureless when the surface roughness was investigated with microscope.

Specimens C: After polishing on the series of the five abrasive-papers, some specimens were polished by an abrasive of 0.3 μm Al_2O_3 in a wet condition. "Comet-tails" were observable with a microscope.

In the discussion below, the polishing procedure for a used specimen will be distinguished by A, B or C.

III-2 Implantation of Deuterium

Polished aluminium-specimens were implanted with D^+ ions of 100 or 200 keV using the Cockcroft-Walton accelerator at The Radiation Laboratory of Kyoto University. The target was kept at around -130°C by liquid nitrogen. A change of the depth profile of deuteriums implanted in aluminium has never been observed at this temperature. The D^+ beam for the implantation was collimated with a 6 mm-dia. aperture. After the implantation of deuterium, samples were stored in liquid nitrogen.

III-3 Probing for Depth Profiling

Probing of the implanted samples was performed on the Van de Graaff accelerator at The Radiation Laboratory of Kyoto University. A schematic diagram of the target chamber is given in Fig. 3. The incident beam of ${}^3\text{He}^+$ of 1.1

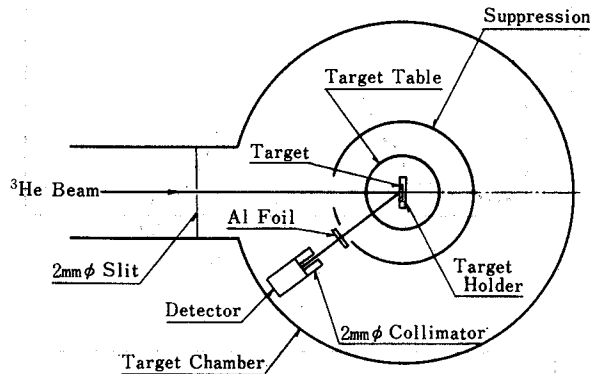


Fig. 3. Schematic diagram of target chamber for probing.

or 1.3 MeV was collimated to 2 mm. A secondary electron shield in the form of a cylinder, with a cap on top, encloses the sample holder. This suppression shield was maintained at -300V . The exit port for the reaction proton was covered with $17\ \mu\text{m}$ aluminium-foil to protect the detector from flooding by backscattered ${}^3\text{He}$ ions and secondary electrons. Samples were kept at around -120°C by liquid nitrogen. To prevent the implanted deuterium from dispersing due to heating by the ${}^3\text{He}$ beam, the current of the probing beam was maintained under $0.1\ \mu\text{A}$.

A silicon detector with a depletion depth of $1500\ \mu\text{m}$ was placed at an angle θ ($=150^\circ$) with respect to the incident beam and collimated to 2 mm diameter. The checking source of ${}^{241}\text{Am}$ was set at the side of the cylinder surface. Before and after probing by the ${}^3\text{He}^+$ beam, it was used for energy calibration of a multi-channel pulse height analyzer (MPHA).

IV. Results and Discussion

IV-1 On Samples Finished by Abrasive Paper (A) or Diamond Paste (B)

A proton energy spectrum obtained for a sample polished only by abrasive papers (A) which was implanted with 100 keV deuterium at the dose of $10^{17}(\text{D}/\text{cm}^2)$ is shown in Fig. 4-a. The energy of the probing ${}^3\text{He}^+$ beam was 1.1 MeV. A peak appears around the energy of 12.75 MeV, which corresponds to a depth of $\sim 0.9\ \mu\text{m}$.

One might think that the probing ions might cause a radiation enhanced

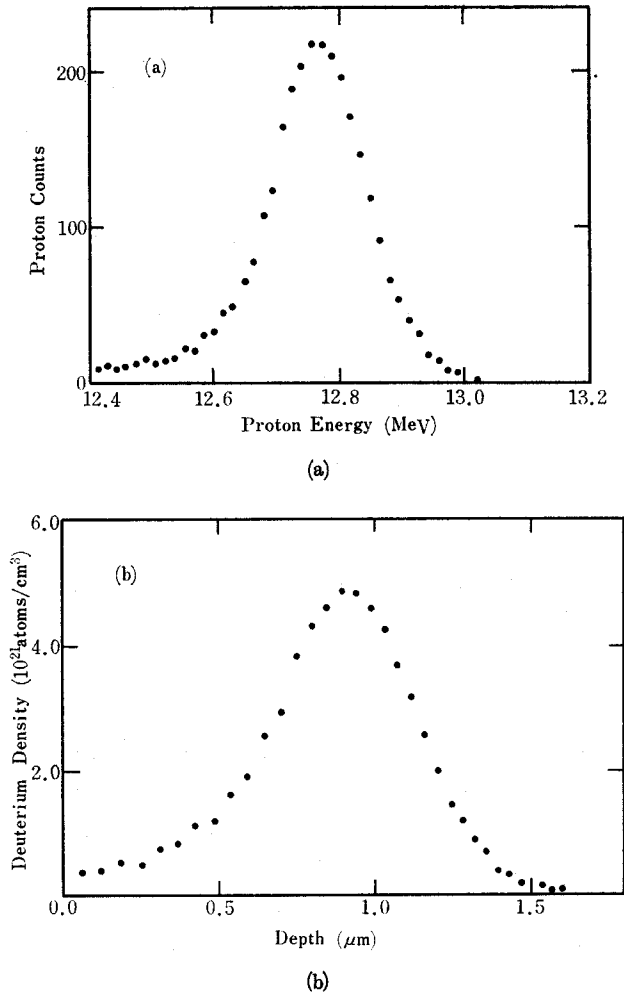


Fig. 4. An example of the results of depth profiling. (a) is plotted on an energy scale and (b) on a depth scale. (D-implantation: $1 \times 10^{17} \text{cm}^{-2}$ at 100 keV, ^3He energy: 1.1 MeV, Polishing: A.)

diffusion of the implanted atoms. However, no changes were found when measuring two energy spectra of the same area of the implanted surface in succession. It may be explained by the fact that radiation damage is produced mainly near the end of the range of the probing ions.

According to the monograph by Ziegler, the projected range of D^+ ions of 100 keV in aluminium is about $0.9 \mu\text{m}$, which is in a fair agreement with the depth of the center of the depth-profile. Bohr's formula²³⁾ or the LSS theory²⁴⁾ has generally been used to estimate the full width at half-maximum (FWHM) in a

profile of implanted particles. However, the deuterium energy of 100 KeV in the present case is so low that the Bohr formula or LSS theory might be applicable only for a crude estimation. The application of the LSS theory leads to $0.3 \mu\text{m}$ of FWHM¹⁹⁾, which is narrower than that in Fig. 4-b. It is thought that the energy-struggling of ^3He , the resolution of the detector, the geometry of the probing system and others contribute to the broadening of the peak. However, the obtained peak-area must be close to the real one.

The depth profile changed with time, as shown in Fig. 5, when the sample

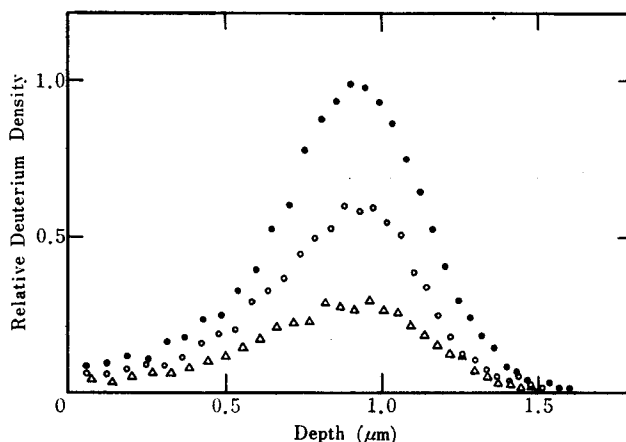


Fig. 5. Effect of annealing at 0°C on the depth profile. (●: Before annealing, ○: Annealed for 2hr, △: Annealed for (2+4) hr. D -implantation: $1 \times 10^{17} \text{ cm}^{-2}$ at 100 keV, ^3He energy: 1.1 MeV, Polishing: A.)

was maintained at 0°C in an evacuated condition. If the dispersion of deuterium had occurred in homogeneous media, the Gaussian profile should have changed, as shown in Fig. 6. Its standard deviation, ω , would increase with time as

$$\omega(t) = \sqrt{\omega_0^2 + 2\mathcal{D}t} \quad (14)$$

where ω_0 is the standard deviation at $t=0$, and \mathcal{D} is the diffusivity of deuterium. The standard deviation ω of a Gaussian is related to FWHM as $\text{FWHM} = 2.355 \cdot \omega$. As seen in Fig. 5, however, the sequential change of profile, observed for the sample and finally polished by the abrasive papers (A), was quite different from that shown in Fig. 6. The FWHM did not increase with time. As discussed by Bugeat and Ligeon²⁵⁾, it seems that implanted deuteriums suffer from a trapping action in an aluminium matrix at the points of the end of the range. Once they are released from the trapping sites, they rapidly disperse over the bulk of aluminium with an ordinary diffusivity measured by permeation methods²⁶⁾.

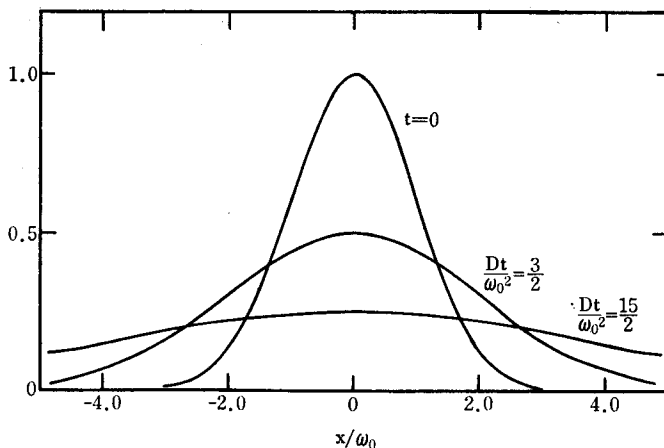


Fig. 6. Change of Gaussian profile due to simple diffusion in homogeneous media. The standard deviation increases with time.

Assuming that the number of deuteriums in the trapped state is expressed by

$$m = m_0 e^{-\lambda t} \tag{15}$$

the time-dependence of the profile in Fig. 5 may be explained qualitatively. In the above expression, for a first-order reaction, m is the number of deuteriums at a trapped state at a time t , m_0 is m at $t=0$, and λ is a constant. The decreasing rate of m leads to an estimation of $\lambda=5 \times 10^{-5}$ (1/sec). It corresponds to 1.4×10^4 sec of the half-life of the trapped state at 0°C .

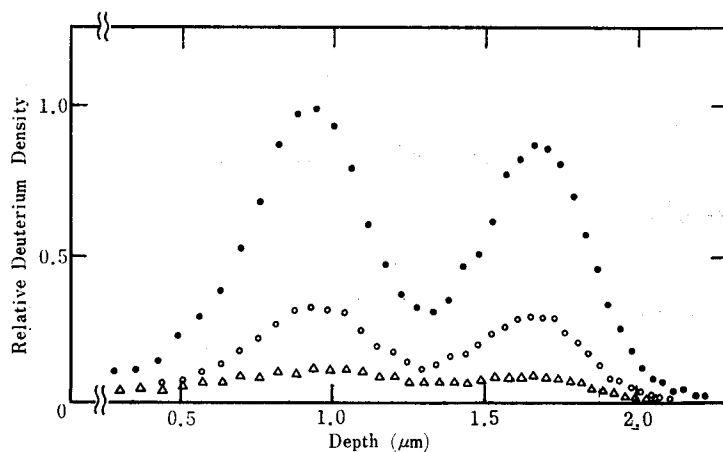


Fig. 7. Effect of annealing at 0°C on the depth profile in double-implanted sample. (D -implantation: $1 \times 10^{17} \text{cm}^{-2}$ at 100 and 200 keV, ^3He energy: 1.3 MeV, \bullet : Before annealing, \circ : Annealed for 2hr, \triangle : Annealed for (2+6)hr, polishing: B.)

A specimen finished by diamond-paste (B) was implanted sequentially at 200 and 100 keV with an equal dose of 1×10^{17} (D/cm²). After analyzing the depth profile, it was maintained at 0°C for 2 hours, and then 6 hours in an evacuated condition.

The observed profiles in the sample before and after the annealing at 0°C are shown in Fig. 7. As seen in this figure, two peaks showed a similar decrease with time. Deuteriums implanted in aluminium specimens A or B dispersed so easily that their behavior at high temperature could not be followed.

IV-2 On Samples finished by Al₂O₃ (C)

Experiments similar to those for the sample polished by abrasive papers (A) or diamond-paste (B) were also performed for samples finished by Al₂O₃ (C). Deuteriums implanted in these samples had a very small dispersibility in comparison to those implanted in samples finally polished by abrasive papers (A) or diamond-paste (B). The change of depth-profile was not detected even when they were kept at room temperature for a few weeks. It is quite certain that something other than the trapping effect discussed in IV-1 controlled the mobility of the deuteriums implanted in specimens finished by Al₂O₃ (C).

Observed profiles before and after annealing for 4 hours at 200°C are shown in Fig. 8. Deuteriums were implanted at energy of 200 keV. As seen in Fig. 8, the FWHM broadened with time in contrast to the cases for samples polished with abrasive papers (A) or diamond-paste (B). (cf. Fig. 5) By using Eq. (14), a rough

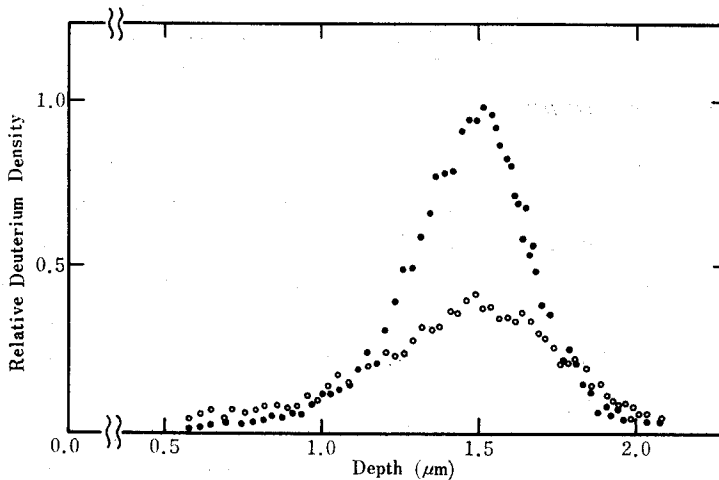


Fig. 8. Effect of annealing at 200°C on depth profile. The FWHM was expanded by annealing. (●: Before annealing, ○: annealed at 200°C for 4hr, D-implantation: 1×10^{17} cm⁻² at 200 keV, ³He energy: 1.3 MeV, Polishing: C.)

estimate of the diffusivity of deuterium at a given temperature can be made.

Diffusivities at 250 and 300°C were also obtained through the same procedure. The Arrhenius plots are given in Fig. 9. It may be expressed by

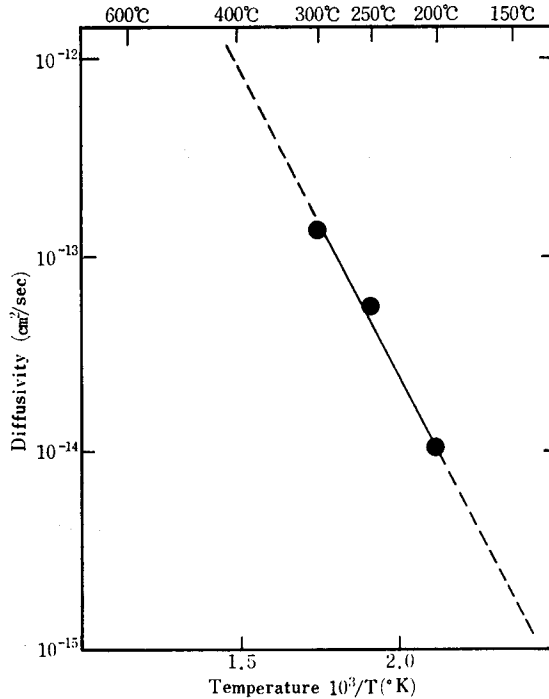


Fig. 9. Arrhenius plots for diffusivity of deuterium implanted in aluminium. (*D*-implantation: $1 \times 10^{17} \text{ cm}^{-2}$ at 200keV, Polishing: C.)

$$D \sim 1.5 \times 10^{-8} e^{-13000/RT} \quad (16)$$

In Fig. 10, the diffusivity expressed by Eq. (16) is compared with previous data²³⁻²⁶ which have been measured by permeation methods. As shown in Fig. 10, the diffusivity of deuterium implanted in the sample finished by Al_2O_3 (C) is much smaller than the extrapolated values of the previous data for deuteriums absorbed in bulk of aluminium. Because the temperature in the present experiment is much lower than those in previous data, a direct comparison of the present results with the extrapolated values of the previous data may not be appropriate. However, it is interesting that the obtained activation energy of diffusion (i.e. the slope in the Arrhenius plots) is nearly equal to those in some of the previous data, and the pre-exponential factor (or frequency factor) is much smaller. According to well-established theories^{26,27,28} on interstitial diffusion, it is almost impossible that the pre-exponential factor be as small as 1.5×10^{-8} for

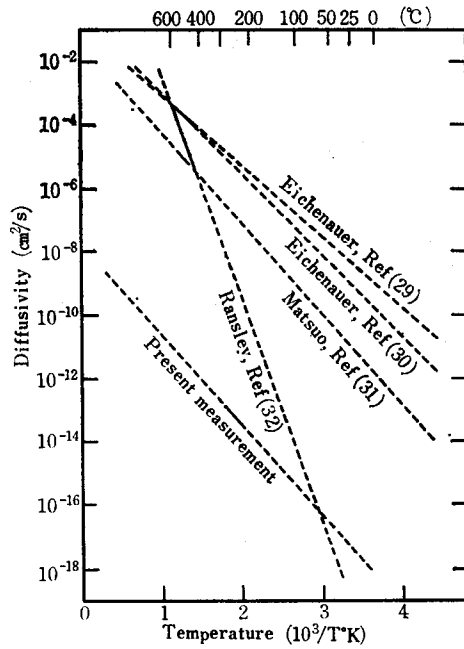


Fig. 10. Comparison of the present result corresponding to Fig. 9 with previous data obtained by permeation methods. (Extrapolations of data are shown by broken lines.)

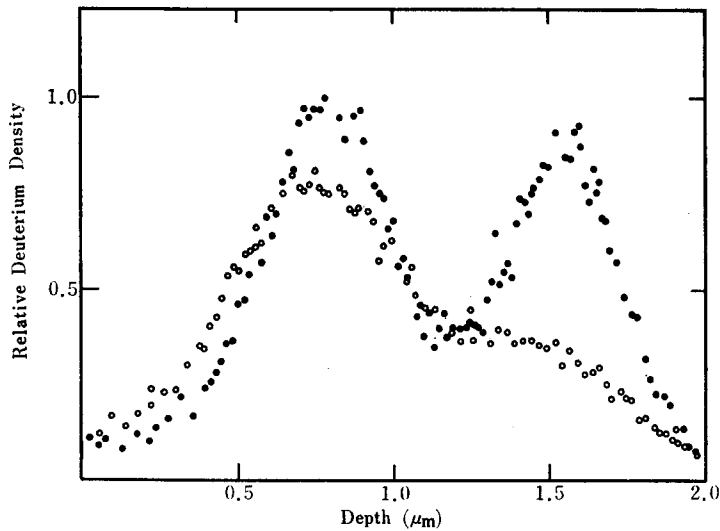


Fig. 11. An example of depth-dependence of dispersion behavior of deuterium. (●: Before annealing, ○: annealed at 200°C for 1hr, D -implantation: $1 \times 10^{17} \text{ cm}^{-2}$ at 100 and 200 keV, ^3He energy: 1.3 MeV, Polishing: C. c.f. Fig. 7.)

hydrogen diffusion in aluminium.

Aluminium specimens finished by Al_2O_3 (C) were implanted with deuteriums sequentially at 200 and 100 keV with an equal dose of 1×10^{17} (D/cm²). Fig. 11 shows one of results of probing before and after their annealing. During the annealing, the peak-height at the deeper location was considerably lower, but that at the location closer to surface was almost unchanged. It shows that the diffusivity of deuteriums depends on the depth. Comparing Fig. 11 with Fig. 7, one may see that the deuterium behavior in specimens finished by Al_2O_3 (C) is quite different from that observed for specimens finished by diamond paste (B) (or five abrasive papers (A)).

We have no physical explanation on the remarkable difference of deuterium-behavior caused by polishing procedures.

V. Conclusion

Applying the depth-profiling technique by use of the nuclear reaction $\text{D}(^3\text{He}, \text{p})^4\text{He}$, the thermal behavior of deuteriums implanted in aluminium at the depth of 0–2 μm were examined. The existence of a weak trapping effect against implanted deuteriums around the end of the range was suggested through the observed thermal-behavior (Fig. 5 and 7). The half-life of the trapped state was estimated as 1.4×10^4 sec at 0°C.

It was found that the thermal behavior near the surface depends greatly on preparation procedures of the samples. The dependency of dispersibility on depth was observed in the case of samples polished with coarse Al_2O_3 (Fig. 11).

Acknowledgment

The authors wish to thank Dr. M. Sakisaka, Mr. S. Kanazawa and the staff of The Radiation Laboratory of Kyoto University for their helpful discussion on the experiments. Also, they wish to thank Dr. M. Umemoto, Mr. T. Yashiki and the staff of The Department of Metal Processing of Kyoto University for the preparation of aluminium samples as well as their valuable discussion on metallography.

The numerical calculations were performed by the computers at The Data Processing Center and The Educational Center for Information Processing of Kyoto University.

References

- 1) J.C. Davis *et al.*: Nucl. Instr. Meth., **149**, 41 (1978).
- 2) E. Ligeon and A. Guivarc'h: Rad. Eff., **22**, 101 (1974).

- 3) E. Ligeon and A. Guivarc'h: *ibid.*, **27**, 129 (1976).
- 4) Y.Y. Chu and L. Friedman: *ibid.*, **38**, 254 (1965).
- 5) C.M. Bartle *et al.*: *ibid.*, **95**, 221 (1971).
- 6) P.B. Johnson: Nucl. Instr. Meth., **114**, 467 (1974).
- 7) W. Möller, M. Hufshmidt and D. Kamke: *ibid.*, **140**, 157 (1974).
- 8) R.A. Langley, S.T. Picraux and F.L. Vook: J. Nucl. Mater., **53**, 257 (1974).
- 9) P.P. Pronko and P.G. Pronko: Phys. Rev., **B9**, 2870 (1974).
- 10) W. Möller, P. Borgessen and J. Bottiger: J. Nucl. Mater., **76 & 77**, 287 (1978).
- 11) W. Möller, and J. Bottiger: *ibid.*, **88**, 95 (1980).
- 12) S.T. Picraux and F.L. Vook: *ibid.*, **53**, 246 (1974).
- 13) D.A. Leich and T.A. Tombrello: *ibid.*, **108**, 67 (1973).
- 14) F.J. Clark *et al.*: Nucl. Instr. Meth., **149**, 9 (1978).
- 15) W.A. Lanford: *ibid.*, **149**, 1 (1978).
- 16) W.A. Lanford *et al.*: Appl. Phys. Lett., **28**, 566 (1976).
- 17) R.E. Beneuseon, L.C. Feldman and B.G. Bagley: Nucl. Instr. Meth., **168**, 547 (1980).
- 18) C.F. Williamson, J.P. Boujot and J. Picard: "Tables of Ranges and Stopping Power of Chemical Elements for Charged Particles of Energy 0.05 to 500 MeV", CEA R-3042 (1966).
- 19) J.E. Ziegler: "Helium Stopping Powers and Ranges in All Elemental Materials", Pergamon Press, London (1977).
- 20) T.W. Bonner, J.P. Conner and A.B. Lillie: Phys. Rev., **88**, 473 (1953).
- 21) J.L. Yarnell, R.H. Lovberg and W.D. Stratton: *ibid.*, **90**, 292 (1953).
- 22) J.R. Lamarsh: "Introduction to Nuclear Reactor Theory", Addison-Welsey P. Company, Massachusetts (1966).
- 23) N. Bohr and K. Dan: Vidensk. Selsk. Mat.-Fys. Medd., **18** 8 (1948).
- 24) J. Lindhard, M. Scharff and H.E. Schiott: Kgl. Danske. Vidensk. Mat.-Fys. Medd., **33**, No. 14 (1963).
- 25) J.P. Bugeut and W. Ligeon: Phys. Lett., **71A**, 93 (1979).
- 26) A.S. Nowick and J.J. Burton: "Diffusion in Solids-Recent Developments", Academic Press, New York (1972).
- 27) C. Zener: "Imperfections in Nearly Perfect Crystals", John Wiley, New York (1975).
- 28) P.G. Shewmon: "Diffusion in Solids", McGraw-Hill, New York (1963).
- 29) W. Eichenauer and A. Pebler: Z. Metallk., **48**, 373 (1957).
- 30) W. Eichenauer: Mem. Sci. Rev. Met., **57**, 943 (1960).
- 31) S. Matsuo and T. Hirata: Nippon Kinzoku Gakkaishi, **31**, 590 (1967).
- 32) C.E. Ransley and D.E.J. Talbot: Z. Metallk., **46**, 328 (1955).